

CMSN: Continuous Multi-stage Network and Variable Margin Cosine Loss for Temporal Action Proposal Generation

Yushuai Hu¹ Yaochu Jin^{1,2} Runhua Li¹ Xiangxiang Zhang¹

¹Ulucu AI Research ²University of Surrey

{hyshuai,lrhua,zxxiang}@ulucu.com, yaochu.jin@surrey.ac.uk

November 21, 2019

Abstract

Accurately locating the start and end time of an action in untrimmed videos is a challenging task. One of the important reasons is the boundary of an action is not highly distinguishable, and the features around the boundary are difficult to discriminate. To address this problem, we propose a novel framework for temporal action proposal generation, namely Continuous Multi-stage Network (CMSN), which divides a video that contains a complete action instance into six stages, namely Background, Ready, Start, Confirm, End, Follow. To distinguish between Ready and Start, End and Follow more accurately, we propose a novel loss function, Variable Margin Cosine Loss (VMCL), which allows for different margins between different categories. Our experiments on THUMOS14 show that the proposed method for temporal proposal generation performs better than the state-of-the-art methods using the same network architecture and training dataset.

1 Introduction

In recent years, with the development of deep learning, classification accuracy of action recognition on trimmed videos has been significantly improved [10, 33, 34]. But real-world videos are usually untrimmed, making location and action classification in untrimmed videos increasingly important. This task named Action Detection aims to identify the action class, and accurately locate the start and end time of each action in untrimmed videos.

By definition, action detection is similar to object detection. While object detection aims to produce spatial location in a 2D image, action detection aims to produce temporal location in a 1D sequence of frames. Because of the similarity between object and action detection, many methods for action localization are inspired from advances in object detection [13, 25], which first generate temporal proposals and then classify each proposal. However, the performances of these methods remain unsatisfactory. As found in the previous work [3, 26, 36, 5], this can mainly be attributed to the different properties between action detection and object detection. For example, the duration of action instances varies a lot, from one second to a few hundred seconds [5], and video streaming always contains a lot of information that is not related to the action, making action detection still a challenging problem.

Because the generation of high-quality proposals is the basis for improving detection performance, in this paper, we mainly focus on the temporal proposal generation. We observe that at the start and end of an action, the action is continuous and does not suddenly start or end. So we believe the probability of the start and end time should not be predicted separately, but should be linked to the front and back to form a continuous sequence of features.

We propose a Continuous Multi-stage Network (CMSN), and its architecture is illustrated in Fig. 1. As shown in the figure, we designed six stage categories based on the video process, and directly predict the category of each frame. The main contributions of our work are two-folds:

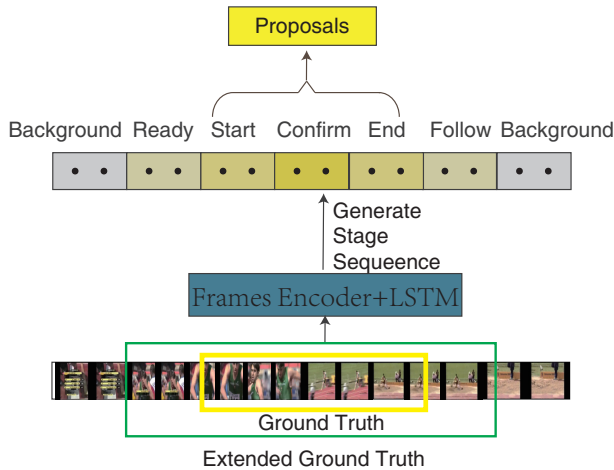


Figure 1: The architecture of our method, firstly we expand the Ground Truth, secondly, the network encodes the frames and generates the action stage categories sequence, finally combines action stages to generate proposals.

- 1) We introduce a new model, CMSN, which expands a complete action instance and divides it into six stages, namely Background, Ready, Start, Confirm, End, Follow, corresponding to background, a short period before the start, a short period after the start, the middle stage, a short period before the end, a short period after the end, and consider six stages as six categories. Then each action instance could be considered as a continuous category sequence, and the categories around the start and end time are separated. This strategy could improve recall performance and location accuracy, and could handle large variations in action duration to some extent.
- 2) In order to locate the start and end time of an action instance more accurately, we propose a new loss function, termed Variable Margin Cosine Loss. The loss function adds a variable angular margin between different classes, which allows similar samples to keep a certain margin and dissimilar samples to have a large margin.

2 Related work

Temporal action detection task focuses on predicting action classes, and temporal boundaries of action instances in untrimmed videos. Most action detection methods are inspired by the success of image object detection [25, 24, 20]. The mainstream methods can be divided into two types, one is a two-stage pipeline [27, 37, 5, 40, 6], and the other is a single-shot pipeline [2, 18, 39]. For the two-stage pipeline, the first step is to generate proposals, and the second step is to classify proposals. According to the findings of previous work, under the same conditions, the two-stage method performs better than the single-shot method.

In a proposal generation task, earlier work [16, 23, 32] mainly use sliding windows as candidates. Recently, many methods [12, 27, 37, 5] use preset fixed-time anchors to generate proposals. TAG [40] divides an activity instance into three stages, then uses an actionness classifier to evaluate the binary actionness probabilities. SMS [38] assumes that each temporal window begins with a single start frame, followed by one or more middle frames, and finally a single end frame. BSN [19] locates temporal boundaries with high probabilities, then evaluate the confidences of candidate proposals generated by these boundaries. BMN [17] proposes the Boundary-Matching mechanism to evaluate confidence scores of densely distributed proposals. MGG [22] proposes a multi-granularity generator to generate temporal action proposals from different granularity perspectives.

Different from the above-mentioned work, we use six stages to represent a complete action instance. Each stage corresponds to a period of an action rather than a frame. We do not just predict the probability of a frame, but predict an action as a continuous multi-stage sequence.

3 Proposed Approach

We propose a novel network for generating proposals in continuous untrimmed video streams, namely Continuous Multi-stage Network (CMSN). As shown in Fig. 2, CMSN takes a video as input, outputs a sequence of action stage categories after Action stage Subnet, and outputs a set of proposals for the input video in the last network. Next, we describe Feature Extractor Subnet (FES)

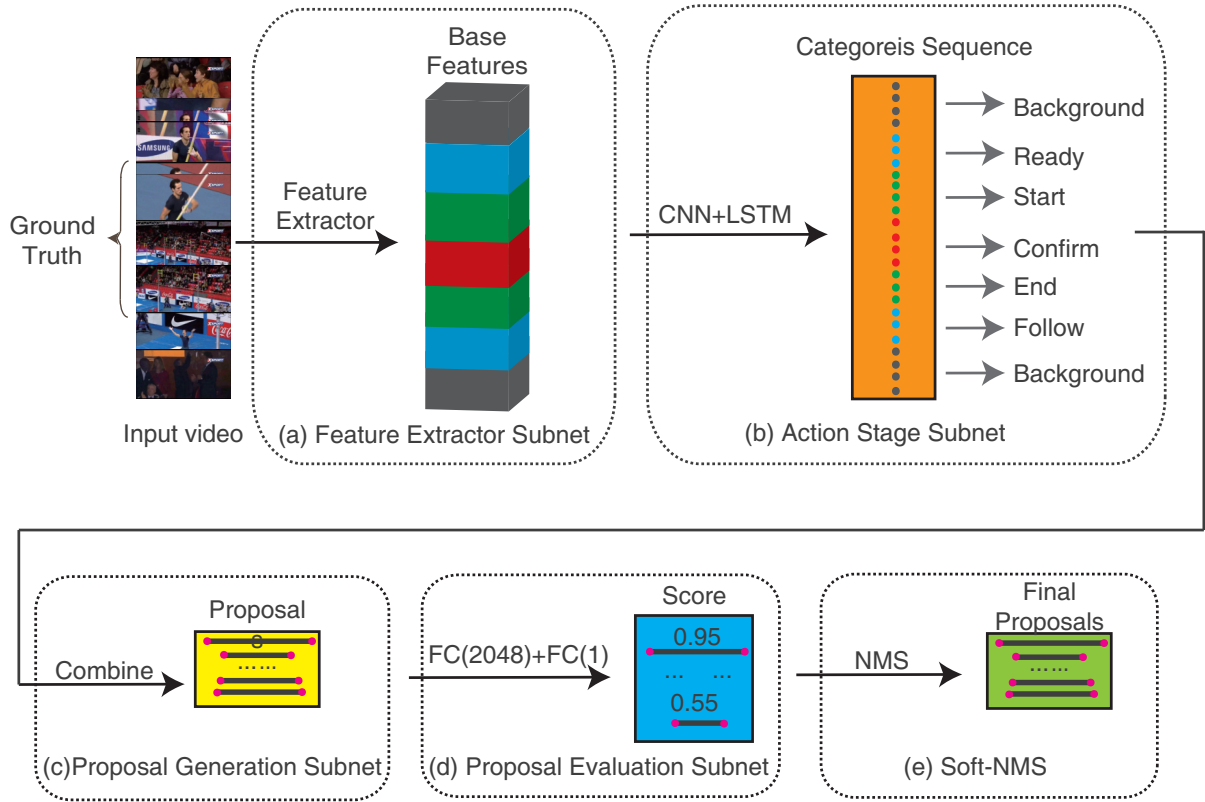


Figure 2: The model architecture. (a) Feature Extractor Subnet (FES) is used for computing feature sequences. (b) The Action Stage Subnet (ASS) takes the features sequence as input, and generates action stage categories sequence corresponding to the input. (c) Proposal Generation Subnet (PGS) combines the action stage sequence to generate proposals and sample features from the features sequence. (d) Proposal Evaluation Subnet (PES) evaluates the IoU of each proposal directly. (e) Soft-NMS

and Action Stage Subnet (ASS) in Section 3.1, Proposal Generation Subnet (PGS) in Section 3.2, Proposal Evaluation Subnet (PES) and Soft NMS in Section 3.3.

3.1 Feature Extractor Subnet and Action Stage Subnet

Suppose the input video frames $\mathcal{V} = \{V_1, \dots, V_t, \dots, V_n\}$, have dimension $[3 \times L_i \times H_i \times W_i]$, where V_t denotes the frame at time step t , and n is the total number of frames in the video. Let $P_i = \{P_s, P_e\}$ denote a proposal, P_s is the start time and P_e is the end time, thus the duration of P_i is $d_i = P_e - P_s$. To make

full use of the context information, we expand the start time P_s to $P'_s = P_s - d_i/2$, and expand the end time P_e to $P'_e = P_e + d_i/2$, as done in [40], but we also divide P_i into three segments by 2 time $(P_s + d_i/3, P_e - d_i/3)$: $A = (P_s, P_s + d_i/3)$, $B = (P_s + d_i/3, P_e - d_i/3)$, $C = (P_e - d_i/3, P_e)$. In this way, the expanded proposal is divided into 5 segments: $\{P'_s, P_s\}$, $\{P_s, P_s + d_i/3\}$, $\{P_s + d_i/3, P_e - d_i/3\}$, $\{P_e - d_i/3, P_e\}$, $\{P_e, P'_e\}$, which corresponds to Ready, Start, Confirm, End, Follow, respectively. And with the stage of background, we have six action stage categories: Background, Ready, Start, Confirm, End, Follow. So each frame of the input video corresponds to one of the six action stage categories.

Feature Extractor Subnet To extract features from a given video, we could use various convolutional networks for action recognition. In our framework, we adapt C3D network [30] as FES. For studying the effect of different video features, the two-stream network [28] will also be experimented. Take the C3D as an example, the input of FES is RGB frames. The input frames \mathcal{V} with dimension $[3 \times L_i \times H_i \times W_i]$ are input into FES and output base features. The output features have dimension: $[C_o \times L_o \times H_o \times W_o]$, with the length, width, height being scaled to the original input frames by the network. Suppose the scale of FES on the dimension length is s_c , then $L_o = L_i/s_c$.

Action Stage Subnet As shown in Fig. 2, ASS consists of a CNN network and a LSTM network. The CNN network scales the base features so that they are suited for the LSTM network, containing two convolutional network layers with a kernel size 3 and hidden size 512, and one max-pooling layer. The outputs of the CNN network have a size $[L_c \times L_o]$, where L_c is the input channel of the LSTM network. The LSTM network which we used is a bidirectional LSTM [14] having 2 layers, which can make use of the context information to a maximum extent. The outputs of the CNN network feed into the LSTM network, then pass through the classification layer. The final output is an action stage categories sequence. Let $Q = [q_1, q_2, \dots, q_n]$ be the output sequence, where $n = L_o$. Because the output length L_o is scaled, the frame-level action stage category also needs to be scaled down by the same ratio s_c .

The reason why we divide the proposal into six segments is based on the following observations. Firstly an action never happens suddenly in a continuous video stream. For example, Billiards, before the action starts, the player must move close to the pool table and adjust the position. Secondly, many actions could not be confirmed to happen in a short period after starting, but need to observe for a while. For example, Long Jump, in the run upstage, one could not distinguish whether the action instance is Long-distance or Long jump. Similarly, before an action ends, we often can predict whether an action is coming to an end. That is, the start stage, the middle stage and the end stage of an action often are distinguishable. Thus, we argue that dividing an action into three stages could more effectively describe the action than one stage, and superadding the Ready and Follow stage could more

effectively make use of the context information.

We do not just predict the probability of a certain moment, such as the start time, but predict the whole action process and model an action instance as a sequence of action stage categories. In this way, the sequence is continuous as a piece of video, so if an intermediate time instead of the start and end time is detected, we can still estimate the start and end time. The categories around the start and end time are separated, so we can control the margin between them as described in Section 4.2.

3.2 Proposal Generation Subnet

The output of the Action Stage Subnet is an action categories sequence Q , which is arranged in the order from Ready to Follow. This corresponds well with the ground truth, but sometimes the order may be erroneous. In the subsequence of the sequence Q , let $Q_r = [r_1, r_2, \dots, r_n]$ denote the Ready sequence, $Q_s = [s_1, s_2, \dots, s_n]$ denote the Start sequence, $Q_c = [c_1, c_2, \dots, c_n]$ denote the Confirm sequence, $Q_e = [e_1, e_2, \dots, e_n]$ denote the End sequence, $Q_f = [f_1, f_2, \dots, f_n]$ denote the Follow sequence. As shown in Fig. 3, we choose start and end locations, and combine them as candidate proposals as follows:

- 1) We choose a location t as start location, if t belongs to Q_r or Q_s or the first half of Q_c . Then we could obtain candidate start point sets $C_s = \{r_1, \dots, s_1, \dots, c_1, \dots, c_{n/2}\}$.
- 2) We choose location t as end location, if t belongs to Q_e or Q_f or the second half of Q_c . Then we could obtain candidate end point sets $C_e = \{c_{n/2}, \dots, c_n, \dots, e_1, \dots, f_1, \dots\}$.
- 3) We combine a start location belonging to C_s and an end location belonging to C_e , if it contains at least one of Start stage and Confirm stage and Follow stage from the start to the end (excluding the Background stage). Finally, we could obtain the candidate proposal point sets $C_p = \{(r_1, c_n), \dots, (r_1, e_1), \dots, (s_1, f_1), \dots, (c_1, c_n), \dots\}$.

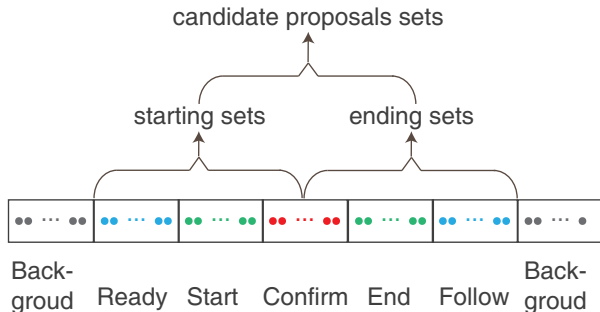


Figure 3: Pipeline of our candidate proposals generation, from action stage categories sequence to candidate proposals sets.

3.3 Proposal Evaluation Subnet and Soft NMS

The input features of PES is the output of the CNN in ASS with size $[L_c \times L_o \times 1 \times 1]$, we intercept the features sequence by the candidate proposal set P_s , and obtain features sets $P(f)$. Because features in $P(f)$ have different lengths, we use RoI pooling [37] to extract the fixed-size volume features. The output of the RoI pooling is fed into two fully connected layers with a hidden size 2048, and output the score corresponding to set $P(f)$.

Because the outputs of ASS could correspond well with the ground truth, we set a preset score for each proposal. Let q_c denote a sequence from Ready to Follow, q_s denote the first Start in the sequence, q_e denote the last End. For a proposal generated from the sequence q_c , let d_s denote the distance between the start of the proposal and q_s , d_e denote the distance between the end of the proposal and q_e . Then we could compute the pre-score as follows:

$$pre-score = (1 - d_s \times i) \times (1 - d_e \times i) \quad (1)$$

where i is the decay rate. Then for each proposal, we use the product of the output score of PES and the pre-score as the final score. Finally, we use non-maximum suppression (NMS) [1] to remove redundant proposals.

3.4 Training and Prediction

Training We train the Action Stage Subnet firstly. For an input video \mathcal{V} , we need to assign labels to the ac-

tion stage categories sequence of ASS. We use ground-truth to generate action stage category labels described in Section 3.1. Because the ground-truth is at frame level, suppose the scale ratio is s_c , as described in Section 3.1. We firstly generate frame-level categories sequence, then sample the sequence at s_c fps to generate label sequence corresponding to action stage categories sequence. The used loss function is Variable Margin Cosine Loss, the categories are assigned to 0–6 corresponding to the stages from Background to Follow. After Action Stage Subnet is trained, we could generate proposals described in Section 3.1. Then we select proposals by Intersection-over-Union (IoU) with some ground-truth activity as follows: firstly select all proposals with IoU higher than 0.6 as Big, suppose the number of Big is n ; secondly, select proposals with IoU higher than 0.2 and lower than 0.6 with the same number n as Middle; finally, select proposals with IoU lower than 0.2 with the number n as Smaller. Then train the IoU Evaluation Subnet with Smooth L1 loss [13].

Prediction For a video to be predicted, we first sample to generate some frames sequences with the same length in training L_i , then we could generate action stage categories sequence with the architecture described in Section 3.1. Because a complete proposal may be truncated at the beginning or end of frames sequence, we have half overlap between contiguous sample frames, finally we can generate proposals described in Section 3.2 and Section 3.3.

4 Variable Margin Cosine Loss

4.1 Softmax Loss and Variations

Softmax loss is widely used in classification tasks and can be formulated as follows:

$$L_s = -\frac{1}{m} \sum_{i=1}^m \log \frac{e^{W_{y_i}^T x_i + b_{y_i}}}{\sum_{j=1}^n e^{W_j^T x_i + b_j}}, \quad (2)$$

where x_i denotes the input feature vector of the i -th sample, corresponding to the y_i -th class. $W_j \in \mathbb{R}^d$ denotes the j -th column of the weight vector $W \in \mathbb{R}^{d \times n}$ and $b_j \in \mathbb{R}^n$ is the bias term. The size of mini-batch and the number of class is m and n , respectively. Under binary classification case, the decision boundary of Softmax loss is: $w_1 x + b_1 = w_2 x + b_2$. Obviously, the boundary does

not have a gap between a positive sample and a negative sample. To solve this problem, some variants were proposed, such as CosFace (LMCL) [31], ArcFace [8] and A-softmax [21]. Take LMCL as an example, the loss function is formulated as follows:

$$L_{lmc} = \frac{1}{N} \sum_i -\log \frac{e^{s(\cos(\theta_{y_i,i})-m)}}{e^{s(\cos(\theta_{y_i,i})-m)} + \sum_{j \neq y_i} e^{s \cos(\theta_{j,i})}}, \quad (3)$$

subject to

$$W = \frac{W^*}{\|W^*\|}, x = \frac{x^*}{\|x^*\|}, \cos(\theta_j, i) = W_j^T x_i \quad (4)$$

where N is the number of training samples, s is the scale factor, x_i is the i -th feature vector corresponding to the ground-truth class of y_i , the W_j is the weight vector of the j -th class, and θ_j is the angle between W_j and x_i . The decision boundary is: $\cos(\theta_1) - m = \cos(\theta_2)$.

All these variants have a margin m between positive and negative samples, and could perform well on some classification tasks such as face recognition. But they do not consider the margin value between different negative samples and the same positive sample, that is, the margin is the same for all negative samples and positive samples. There is a similarity relationship between different sample categories, denoted by $S(i, j)$. We define this relationship $S(i, j)$ as the distance between two categories in the sample space, and define the features set for classification as feature space. Then these variations could not maintain the distance $S(i, j)$ when mapped from the sample space to the feature space. We believe that it is unreasonable to use the same margin for positive and negative samples and hypothesize that the margin should vary depending on the distance $S(i, j)$, i.e., the larger $S(i, j)$ is, the larger the margin should be.

4.2 Variable Margin Cosine Loss

To achieve the above goal, we propose the Variable Margin Cosine Loss (VMCL). Formally, let i denote i -th class, j denote j -th class, we define VMCL as follows:

$$L_v = \frac{1}{N} \sum_i -\log \frac{e^{s(\cos(\theta_{y_i,i}))}}{e^{s(\cos(\theta_{y_i,i}))} + \sum_{j \neq y_i} e^{s(\cos(\theta_{j,i})+f(j,i))}} \quad (5)$$

0	1		2	3	4		5	0	1		2	3	4	5	
0	1	2	3	4	5	6	7	8	9	10	11	12	13	14	15

Figure 4: Preset values for different classes, inside the box is the class, and the below is the corresponding value. For example, class 2 corresponds to value 3, 11.

where $f(j, i)$ is variable that determines the margin between i and j . The decision boundary is: $\cos(\theta_i) = \cos(\theta_j) + f(j, i)$. $f(j, i)$ could have various forms as long as it guarantees that $f(j, i)$ is bigger when the distance $S(i, j)$ between i and j is bigger. Without loss of generality, we define $f(j, i)$ as follows:

$$f(j, i) = |v(j) - v(i)| \times m + n \quad (6)$$

where n is the minimum margin, m controls the growth rate of the interval. $v(i)$ is the predefined value of class i . The setting for $v(i)$ is based on the distance $S(i, j)$ between two classes.

When classifying the action stage category, in order to localize the start and end time more accurately, we increase the margin between the ready stage and start stage, end-stage and follow stage. Let 0, 1, 2, 3, 4, 5, 6 denote Background, Ready, Start, Middle, End, Follow, respectively. We preset $v(i)$ as Fig. 4, each category corresponds to one or more values, then we calculate $f(j, i)$ as follows:

$$f(j, i) = \min(|v(j) - v(i)|) \times m + n \quad (7)$$

This setting makes a large margin between Ready and Start, End and Follow. And the setting also makes a bigger margin when the distance between the two stages is bigger. For example, let $m = 0.1$ and $n = 0.15$, the margin between Ready and other stages is $[0.15, 0.0, 0.25, 0.35, 0.45, 0.25]$, which corresponds to stages from Background to Follow.

4.3 Discussions

Compared with Softmax Loss and Variations, VMCL considers the different margin values between different categories, and maps the distance $S(i, j)$ in the sample space to the variable margin $f(j, i)$ in the feature space. And because $f(j, i)$ is variable, we could set a large margin even if the distance $S(i, j)$ is small. VMCL can also

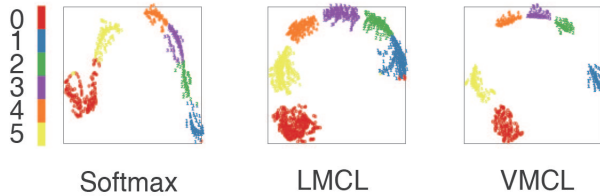


Figure 5: Visualization of features learned with different loss functions. We project the features used in the ASS onto the angular space. 0, 1, 2, 3, 4, 5, 6 denote Background, Ready, Middle, End, Follow, respectively.

have other forms. For example, based on ArcFace, VMCL can be defined as follows:

$$L_v = \frac{1}{N} \sum_i -\log \frac{e^{s(\cos(\theta_{y_i, i}))}}{e^{s(\cos(\theta_{y_i, i}))} + \sum_{j \neq y_i} e^{s(\cos(\theta_{j, i} - f(j, i)))}} \quad (8)$$

the symbols are the same as Equation 5. To better understand the impact of VMCL on classification, we did a pilot study on different loss functions. We take out the features before the classification layer in the ASS and reduce the dimension to the 2-dimensional angular space. As shown in Fig. 5, Softmax does not have a significant margin between the different categories. LMCL has a large margin and the margin is the same. VMCL has a varying margin between different categories. In particular, according to our settings, there is a larger margin between Ready, Follow and Start, End. This distribution makes the features around the start and end time more distinguishable, and theoretically can improve the positioning accuracy.

5 Experiments

5.1 Dataset and Experimental Settings

Dataset We compare our method with the state-of-the-art methods on the temporal action detection benchmark of THUMOS14 [15]. THUMOS14 dataset includes 200 and 213 temporal annotated untrimmed videos with 20 action classes in validation and test sets, respectively. On average, each video contains more than 15 action instances. Because the training set of THUMOS14 contains trimmed videos, so following the settings in previous work, we use

Table 1: Comparisons on THUMOS14 in terms of AR@AN using the C3D network.

Network	Method	@50	@100	@200
C3D	DAPs [9]	13.56	23.83	33.96
C3D	SCNN-prop [26]	17.22	26.17	37.01
C3D	SST [3]	19.90	28.36	37.90
C3D	TURN [12]	19.63	27.96	38.34
C3D	MGG[22]	29.11	36.31	44.32
C3D	BSN+Greedy-NMS[19]	27.19	35.38	43.61
C3D	BSN+Soft-NMS[19]	29.58	37.38	45.55
C3D	BMN+Greedy-NMS[17]	29.04	37.72	46.79
C3D	BMN+Soft-NMS[17]	32.73	40.68	47.86
C3D	CMSN+Greedy-NMS	40.45	46.48	52.23
C3D	CMSN+Soft-NMS	40.40	46.71	52.46

200 untrimmed videos in the validation set to train our model and evaluate on the test set.

Evaluation metrics For the temporal action proposal generation task, Average Recall (AR) calculated with multiple IoU thresholds is typically used as the evaluation metrics. In our experiments, we use the IoU thresholds set [0.5 : 0.05 : 1.0] on THUMOS14. And we also evaluate AR with Average Number of proposals (AN) on THUMOS14, which is denoted as AR@AN.

Implementation details We experiment with two feature extraction methods: C3D network [30] and two-stream network [28]. For the C3D network, our implementation uses RGB frames continuously extracted from a video as input. The length of the input is set to 768, all video frames are resized to 128×171 , then cropped to 112×112 . Since the GPU memory is limited, the mini-batch size is set to 1. So the input dimensions are $1 \times 3 \times 768 \times 112 \times 112$. The FES adopts the convolutional layers (conv1a to conv5b) of C3D [30] pre-trained on ActivityNet-1.3 [4] training set, and freeze the first two convolutional layers. The learning rate is set to 0.0001 and the weight decay parameter is 0.0005, the dropout rate is 0.5. The prescore decay rate is 0.09, n is 0.15, m is 0.1. We first train the Action Stage Subnet for three epochs, then train Iou Evaluation Subnet for four epochs while freezing the Feature Extractor Subnet and the Action Stage Subnet.

For the 2-Stream network, we use the architecture de-

Table 2: Comparisons on THUMOS14 in terms of AR@AN using the 2-Stream network.

Network	Method	@50	@100	@200
Flow	TURN [12]	21.86	31.89	43.02
2-Stream	TAG [36]	18.55	29.00	39.61
2-Stream	CTAP [11]	32.49	42.61	51.97
2-Stream	MGG [22]	39.93	47.75	51.97
2-Stream	BSN+Greedy-NMS[19]	35.41	43.55	52.23
2-Stream	BSN+Soft-NMS[19]	37.46	46.06	53.21
2-Stream	BMN+Greedy-NMS[17]	37.15	46.75	54.84
2-Stream	BMN+Soft-NMS[17]	39.36	47.72	54.70
2-Stream	CMSN+Greedy-NMS	43.24	50.22	56.11
2-Stream	CMSN+Soft-NMS	43.77	50.55	56.48

Table 3: Comparisons of different pre-trained C3D model on THUMOS14 in terms of AR@AN.

pre-trained model	@50	@100	@200
UCF-101	39.87	46.08	52.07
Activitynet	40.40	46.71	52.46

Table 4: Comparison with and without PES on THUMOS14 in terms of AR@AN.

	Network	@50	@100	@200
Without PES	C3D	38.52	42.41	49.35
With PES	C3D	40.40	46.71	52.46
Without PES	2-Stream	39.04	47.13	53.53
With PES	2-Stream	43.77	50.55	56.48

Table 5: Comparisons of different IoU thresholds on THUMOS14 in terms of Recall@AN=100 when using the 2-Stream network.

ASS setting	IoU=0.70	IoU=0.74	IoU=0.8
CNN-LSTM	50.23	50.47	49.57
AvgPool-LSTM	50.38	50.55	49.69

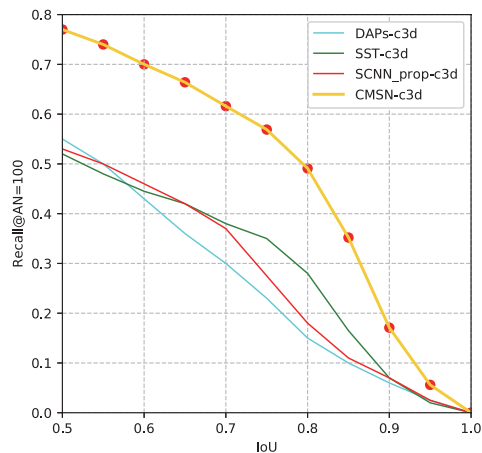


Figure 6: Recall@AN=100 curves of different methods using C3D network on THUMOS14.

scribed in [35]. The network uses BN-Inception as the temporal network, and uses ResNet as the spatial network. We use the network pre-trained on ActivityNet-1.3 [4]. The extracted features are concatenated from the output of the last fully-connected layer, with a dimension of 400. Because the shape of the extract features has changed, we fine-tune the structure of the ASS. We change the CNN in the ASS from two convolutional layers and one max-pooling layer to one average-pooling layer. The rest of the network structure remains unchanged. We first train the Action Stage Subnet for sixteen epochs, then train IoU Evaluation Subnet for sixteen epochs. The other settings are the same as for the C3D network.

5.2 Comparisons

Comparison of AR@AN We first evaluate the average recall performance with numbers of proposals (AR@AN) and area under the AR-AN curve. Table 1 summarizes all comparative results obtained by C3D network on the test set of THUMOS14. It is observed that our method outperforms other methods when AN ranges from 50 to 200. For example, for AR@100, our method improves the performance from the previous record 40.68% to 46.71%. Specifically, for AR@50, our method significantly improves the performance from the previous record 32.73%

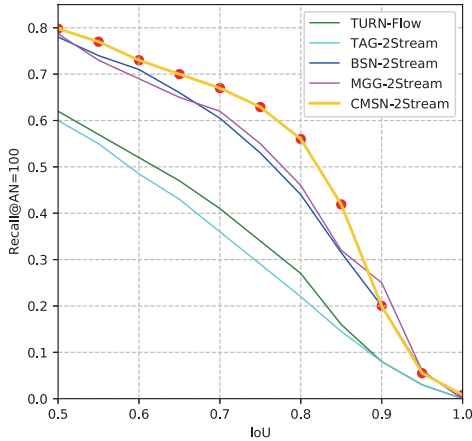


Figure 7: Recall@AN=100 curves of different methods using 2-Stream network on THUMOS14.

to 40.45%, and surpasses the previous results which use the 2-Stream network. Table 2 shows the results using 2-Stream network. It can also be seen that CMSN has the best performance. These results suggest that our method is efficient and does not rely on a specific feature extraction network.

Comparison of different NMS Because most previous work adopted Greedy-NMS [7] for redundant proposals suppression, we also experiment with the effect of different NMS methods on the results. Results in Table 1 and Table 2 show that the results of different NMS methods are comparable, suggesting that our method does not rely on a specific NMS method.

Comparison of AR@AN curves Fig. 6 and Fig. 7 illustrate the Recall@AN=100 curves of different methods on THUMOS14. When using the C3D networks, the performance of our method is significantly better than that of the compared ones. When using the 2-stream network, our method also achieved the best performance. Fig. 8 and Fig. 9 illustrate the average recall against the average number of proposals curve of THUMOS14. It can be seen that our methods have achieved the best performance. Especially in the low AN region, our method shows clear advantages. These results suggest that our method could generate proposals of higher quality.

Comparison of different pre-trained models To more

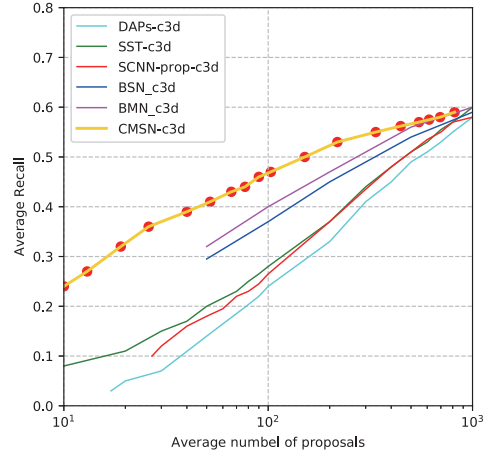


Figure 8: AR-AN curves of different methods using C3D network on THUMOS14.

Table 6: Comparison of the effect of VMCL on THUMOS14 in terms of AR@AN.

	@50	@100	@200
ASS with Softmax Loss	34.73	38.89	42.58
ASS with LMCL [31]	34.82	38.99	42.25
ASS with VMCL	38.52	42.41	49.35

accurately evaluate the effects of our model and the proposed loss function, we present experimental results of CMSN with different pre-trained C3D model in Table 3. In Table 3, UCF-101 denotes the model is pre-trained on UCF-101 [29], Activitynet denotes the model is pre-trained on ActivityNet-1.3 training set. For the C3D model pre-trained on UCF-101, we freeze all convolutional layers (conv1a to conv5b), the other settings are the same as when using the C3D model pre-trained on ActivityNet-1.3. As shown in Table 3, the results of different pre-trained C3D models are very close, suggesting that our method does not depend on a specific pre-trained model.

Comparison with or without PES Table 4 shows the results of CMSN with and without PES, where without PES means that the Proposal Evaluation Subnet and the NMS Subnet are removed. The results without PES are close to adding PES and NMS Subnet. These results suggest that the performance enhancement can mainly be at-

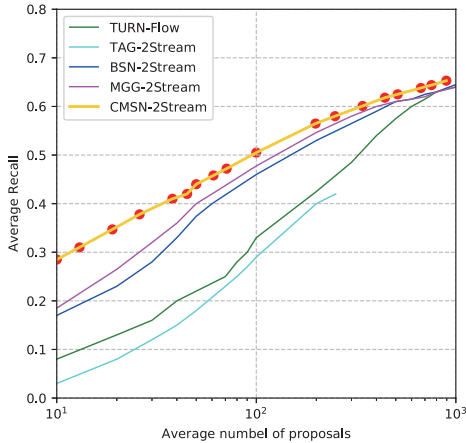


Figure 9: AR-AN curves of different methods using 2-Stream network on THUMOS14.
 Table 7: Comparison different settings of VMCL on THUMOS14 in terms of AR@AN.

n	m	@50	@100	@200
0.1	0.1	37.61	41.85	47.81
0.15	0.1	38.52	42.41	49.35
0.18	0.12	37.83	42.59	48.60
0.25	0.8	37.79	42.30	47.59

tributed to ASS and VMCL.

Comparison different IoU thresholds Table 5 shows the results of different IoU thresholds and different settings. We use the 2-Stream network as the Feature Extractor Subnet. CNN-LSTM means that the CNN of the ASS contains one convolutional layer, Avgpool-LSTM means that the CNN of the ASS contains one avg-pool layer. It can be seen that these results are comparable and both exceed the previous works. These results suggest that our method is robust to configuration of the network.

5.3 Ablative Study for VMCL

To demonstrate the effectiveness of different settings in VMCL, we run several ablations to analyze VMCL. All experiments in this ablation study are performed on the THUMOS14 dataset with the C3D network. And for removing the effect of the Proposal Evaluation Subnet, we only compare the results after removing PES and the Soft-NMS Subnet.

Effect of VMCL Table 6 shows the results of different loss functions. With Softmax Loss, we still get a good result, which suggests that the architecture of ASS is reasonable. With LMCL, we have the same margin between different classes, and the performance of LMCL is worse than VMCL. VMCL performs the best and has significant advantages over other loss functions. These results suggest that ASS is effective and VMCL could achieve better performance.

Effect of m and n Since the parameters m and n of VMCL control the decision boundary, we conduct experiments with different values. As shown in Table 7, the performance is better when $n = 0.15, m = 0.1$ and $n = 0.18, m = 0.12$, and performance degrades when $n = 0.1, m = 0.1$ and $n = 0.25, m = 0.8$. This means that a too small or too large margin will result in performance degradation.

VMCL can also be used for other tasks. For example, when the target probability distribution is in the interval $[0 - 1]$, VMCL can be used to replace the Mean Squared Error. We can consider the probability in the $[0 - 1]$ interval as 100 categories, then we can use Equation 5 and Equation 6 to calculate the classification loss.

6 Conclusions

In this paper, we proposed a Continuous Multi-stage Network (CMSN) and a Variable Margin Cosine Loss (VMCL) for temporal action proposal generation. The CMSN directly predicts the entire sequence of action processes rather than predicting the probability of a frame. The VMCL could arbitrarily adjust the distance between different classes in the feature space. The results on large-scale benchmarks THUMOS14 suggest that our proposed method could significantly improve the location accuracy.

References

- [1] Navaneeth Bodla, Bharat Singh, Rama Chellappa, and Larry S Davis. Soft-nms—improving object detection with one line of code. In *Proceedings of the IEEE international conference on computer vision*, pages 5561–5569, 2017. 5
- [2] Shyamal Buch, Victor Escorcia, Bernard Ghanem, Li Fei-Fei, and Juan Carlos Niebles. End-to-end, single-stream

- temporal action detection in untrimmed videos. In *BMVC*, volume 2, page 7, 2017. 2
- [3] Shyamal Buch, Victor Escorcia, Chuanqi Shen, Bernard Ghanem, and Juan Carlos Niebles. Sst: Single-stream temporal action proposals. In *Proceedings of the IEEE conference on Computer Vision and Pattern Recognition*, pages 2911–2920, 2017. 1, 7
- [4] Fabian Caba Heilbron, Victor Escorcia, Bernard Ghanem, and Juan Carlos Niebles. Activitynet: A large-scale video benchmark for human activity understanding. In *Proceedings of the IEEE Conference on Computer Vision and Pattern Recognition*, pages 961–970, 2015. 7, 8
- [5] Yu-Wei Chao, Sudheendra Vijayanarasimhan, Bryan Seybold, David A Ross, Jia Deng, and Rahul Sukthankar. Rethinking the faster r-cnn architecture for temporal action localization. In *Proceedings of the IEEE Conference on Computer Vision and Pattern Recognition*, pages 1130–1139, 2018. 1, 2
- [6] Xiyang Dai, Bharat Singh, Guyue Zhang, Larry S Davis, and Yan Qiu Chen. Temporal context network for activity localization in videos. In *Proceedings of the IEEE International Conference on Computer Vision*, pages 5793–5802, 2017. 2
- [7] Navneet Dalal and Bill Triggs. Histograms of oriented gradients for human detection. 2005. 9
- [8] Jiankang Deng, Jia Guo, Niannan Xue, and Stefanos Zafeiriou. Arcface: Additive angular margin loss for deep face recognition. In *Proceedings of the IEEE Conference on Computer Vision and Pattern Recognition*, pages 4690–4699, 2019. 6
- [9] Victor Escorcia, Fabian Caba Heilbron, Juan Carlos Niebles, and Bernard Ghanem. Daps: Deep action proposals for action understanding. In *European Conference on Computer Vision*, pages 768–784. Springer, 2016. 7
- [10] Basura Fernando, Efstratios Gavves, Jose M Oramas, Amir Ghodrati, and Tinne Tuytelaars. Modeling video evolution for action recognition. In *Proceedings of the IEEE Conference on Computer Vision and Pattern Recognition*, pages 5378–5387, 2015. 1
- [11] Jiyang Gao, Kan Chen, and Ram Nevatia. Ctap: Complementary temporal action proposal generation. In *Proceedings of the European Conference on Computer Vision (ECCV)*, pages 68–83, 2018. 8
- [12] Jiyang Gao, Zhenheng Yang, Kan Chen, Chen Sun, and Ram Nevatia. Turn tap: Temporal unit regression network for temporal action proposals. In *Proceedings of the IEEE International Conference on Computer Vision*, pages 3628–3636, 2017. 2, 7, 8
- [13] Ross Girshick. Fast r-cnn. In *Proceedings of the IEEE international conference on computer vision*, pages 1440–1448, 2015. 1, 5
- [14] Alex Graves, Santiago Fernández, and Jürgen Schmidhuber. Bidirectional lstm networks for improved phoneme classification and recognition. In *International Conference on Artificial Neural Networks*, pages 799–804. Springer, 2005. 4
- [15] Haroon Idrees, Amir R Zamir, Yu-Gang Jiang, Alex Gorban, Ivan Laptev, Rahul Sukthankar, and Mubarak Shah. The thumos challenge on action recognition for videos in the wild. *Computer Vision and Image Understanding*, 155:1–23, 2017. 7
- [16] Svebor Karaman, Lorenzo Seidenari, and Alberto Del Bimbo. Fast saliency based pooling of fisher encoded dense trajectories. In *ECCV THUMOS Workshop*, volume 1, page 5, 2014. 2
- [17] Tianwei Lin, Xiao Liu, Xin Li, Errui Ding, and Shilei Wen. Bmn: Boundary-matching network for temporal action proposal generation. In *Proceedings of the IEEE International Conference on Computer Vision*, pages 3889–3898, 2019. 2, 7, 8
- [18] Tianwei Lin, Xu Zhao, and Zheng Shou. Single shot temporal action detection. In *Proceedings of the 25th ACM international conference on Multimedia*, pages 988–996. ACM, 2017. 2
- [19] Tianwei Lin, Xu Zhao, Haisheng Su, Chongjing Wang, and Ming Yang. Bsn: Boundary sensitive network for temporal action proposal generation. In *Proceedings of the European Conference on Computer Vision (ECCV)*, pages 3–19, 2018. 2, 7, 8
- [20] Wei Liu, Dragomir Anguelov, Dumitru Erhan, Christian Szegedy, Scott Reed, Cheng-Yang Fu, and Alexander C Berg. Ssd: Single shot multibox detector. In *European conference on computer vision*, pages 21–37. Springer, 2016. 2
- [21] Weiyang Liu, Yandong Wen, Zhiding Yu, Ming Li, Bhiksha Raj, and Le Song. Sphereface: Deep hypersphere embedding for face recognition. In *Proceedings of the IEEE conference on computer vision and pattern recognition*, pages 212–220, 2017. 6
- [22] Yuan Liu, Lin Ma, Yifeng Zhang, Wei Liu, and Shih-Fu Chang. Multi-granularity generator for temporal action proposal. In *Proceedings of the IEEE Conference on Computer Vision and Pattern Recognition*, pages 3604–3613, 2019. 2, 7, 8
- [23] Dan Oneata, Jakob Verbeek, and Cordelia Schmid. The lear submission at thumos 2014. 2014. 2
- [24] Joseph Redmon, Santosh Divvala, Ross Girshick, and Ali Farhadi. You only look once: Unified, real-time object

- detection. In *Proceedings of the IEEE conference on computer vision and pattern recognition*, pages 779–788, 2016. 2
- [25] Shaoqing Ren, Kaiming He, Ross Girshick, and Jian Sun. Faster r-cnn: Towards real-time object detection with region proposal networks. In *Advances in neural information processing systems*, pages 91–99, 2015. 1, 2
- [26] Zheng Shou, Dongang Wang, and Shih-Fu Chang. Temporal action localization in untrimmed videos via multi-stage cnns. In *Proceedings of the IEEE Conference on Computer Vision and Pattern Recognition*, pages 1049–1058, 2016. 1, 7
- [27] Zheng Shou, Dongang Wang, and Shih-Fu Chang. Temporal action localization in untrimmed videos via multi-stage cnns. In *Proceedings of the IEEE Conference on Computer Vision and Pattern Recognition*, pages 1049–1058, 2016. 2
- [28] Karen Simonyan and Andrew Zisserman. Two-stream convolutional networks for action recognition in videos. In *Advances in neural information processing systems*, pages 568–576, 2014. 4, 7
- [29] Khurram Soomro, Amir Roshan Zamir, and M Shah. A dataset of 101 human action classes from videos in the wild. *Center for Research in Computer Vision*, 2012. 9
- [30] Du Tran, Lubomir Bourdev, Rob Fergus, Lorenzo Torresani, and Manohar Paluri. Learning spatiotemporal features with 3d convolutional networks. In *Proceedings of the IEEE international conference on computer vision*, pages 4489–4497, 2015. 4, 7
- [31] Hao Wang, Yitong Wang, Zheng Zhou, Xing Ji, Dihong Gong, Jingchao Zhou, Zhifeng Li, and Wei Liu. Cosface: Large margin cosine loss for deep face recognition. In *Proceedings of the IEEE Conference on Computer Vision and Pattern Recognition*, pages 5265–5274, 2018. 6, 9
- [32] Limin Wang, Yu Qiao, and Xiaoou Tang. Action recognition and detection by combining motion and appearance features. *THUMOS14 Action Recognition Challenge*, 1(2):2, 2014. 2
- [33] Limin Wang, Yu Qiao, and Xiaoou Tang. Action recognition with trajectory-pooled deep-convolutional descriptors. In *Proceedings of the IEEE conference on computer vision and pattern recognition*, pages 4305–4314, 2015. 1
- [34] Limin Wang, Yuanjun Xiong, Zhe Wang, Yu Qiao, Dahua Lin, Xiaoou Tang, and Luc Van Gool. Temporal segment networks: Towards good practices for deep action recognition. In *European conference on computer vision*, pages 20–36. Springer, 2016. 1
- [35] Yuanjun Xiong, Limin Wang, Zhe Wang, Bowen Zhang, Hang Song, Wei Li, Dahua Lin, Yu Qiao, Luc Van Gool, and Xiaoou Tang. Cuhk & ethz & siat submission to activitynet challenge 2016. *arXiv preprint arXiv:1608.00797*, 2016. 8
- [36] Yuanjun Xiong, Yue Zhao, Limin Wang, Dahua Lin, and Xiaoou Tang. A pursuit of temporal accuracy in general activity detection. *arXiv preprint arXiv:1703.02716*, 2017. 1, 8
- [37] Huijuan Xu, Abir Das, and Kate Saenko. R-c3d: Region convolutional 3d network for temporal activity detection. In *Proceedings of the IEEE international conference on computer vision*, pages 5783–5792, 2017. 2, 5
- [38] Zehuan Yuan, Jonathan C Stroud, Tong Lu, and Jia Deng. Temporal action localization by structured maximal sums. In *Proceedings of the IEEE Conference on Computer Vision and Pattern Recognition*, pages 3684–3692, 2017. 2
- [39] Da Zhang, Xiyang Dai, Xin Wang, and Yuan-Fang Wang. S3d: Single shot multi-span detector via fully 3d convolutional networks. *arXiv preprint arXiv:1807.08069*, 2018. 2
- [40] Yue Zhao, Yuanjun Xiong, Limin Wang, Zhirong Wu, Xiaoou Tang, and Dahua Lin. Temporal action detection with structured segment networks. In *Proceedings of the IEEE International Conference on Computer Vision*, pages 2914–2923, 2017. 2, 3